

1 **Within Host Evolution Results in Antigenically Distinct GII.4 Noroviruses**

2 Kari Debbink<sup>a</sup>, Lisa C. Lindesmith<sup>b</sup>, Martin T. Ferris<sup>c</sup>, Jesica Swanstom<sup>b</sup>, Martina  
3 Beltramello<sup>d</sup>, Davide Corti<sup>d,e</sup>, Antonio Lanzavecchia<sup>d,f</sup>, and Ralph S. Baric<sup>a,b,#</sup>

4

5 Department of Microbiology and Immunology, University of North Carolina,

6 Chapel Hill, NC, USA<sup>a</sup>; Department of Epidemiology, University of North

7 Carolina, Chapel Hill, NC, USA<sup>b</sup>; Department of Genetics, University of North

8 Carolina, Chapel Hill, NC, USA<sup>c</sup>; Institute for Research in Biomedicine,

9 Bellinzona, Switzerland<sup>d</sup>; Humabs Biomed SA, Bellinzona, Switzerland<sup>e</sup>; Institute

10 of Microbiology, ETH Zurich, Zurich, Switzerland<sup>f</sup>

11

12 Running Head: Norovirus Within Host Evolution

13 #Address correspondence to Ralph Baric, [rbaric@sph.unc.edu](mailto:rbaric@sph.unc.edu)

14

15

16 Abstract word count: 193

17 Text word count: 5,663

18

19 **Abstract**

20 GII.4 noroviruses are known to rapidly evolve, with the emergence of a new  
21 primary strain every 2-4 years as herd immunity to the previously-circulating  
22 strain is overcome. Because viral genetic diversity is higher in chronic as  
23 compared to acute infection, chronically-infected immunocompromised people  
24 have been hypothesized as a potential source for new epidemic GII.4 strains.  
25 However, while some capsid protein residues are under positive selection and  
26 undergo patterned changes in sequence variation over time, the relationships  
27 between genetic variation and antigenic variation remains unknown. Based on  
28 previously-published GII.4 strains from a chronically-infected individual, we  
29 synthetically reconstructed VLPs representing an early and late isolates from a  
30 small bowel transplant patient chronically infected with norovirus, as well as the  
31 parental GII.4-2006b strain. We demonstrate that intra-host GII.4 evolution  
32 results in the emergence of antigenically distinct strains over time, comparable to  
33 the variation noted between chronologically predominant GII.4 strains GII.4-  
34 2006b and GII.4-2009. Our data suggest that in some individuals the evolution  
35 that occurs during a chronic norovirus infection overlaps with changing antigenic  
36 epitopes that are associated with successive outbreak strains and may select for  
37 isolates that are potentially able to escape herd immunity from earlier isolates.

38 **Importance**

39 Noroviruses are agents of gastrointestinal illness, infecting an estimated 21  
40 million people per year in the United States alone. In healthy individuals,  
41 symptomatic infection typically resolves within 24-48 hours. However, symptoms

42 may persist years in immunocompromised individuals, and development of  
43 successful treatments for these patients is a continued challenge. This work is  
44 relevant to the design of successful norovirus therapeutics for chronically infected  
45 patients, provides support for previous assertions that chronically infected  
46 individuals may serve as reservoirs for new, antigenically unique emergent  
47 strains, and furthers our understanding of GII.4 norovirus immune-driven  
48 molecular evolution.

49

## 50 **Introduction**

51           Noroviruses are the leading cause of gastrointestinal illness worldwide.  
52 While typically an acute disease, norovirus infections can be serious in the  
53 young, old, and immunocompromised, as these groups are at risk for more  
54 severe disease and death (1-3). Norovirus is spread rapidly in environments  
55 where people are found in close proximity including schools and daycares,  
56 nursing homes, cruise ships, and hospitals. Importantly, hospital outbreaks can  
57 result in significant economic damage, with direct and indirect costs from a single  
58 outbreak reaching \$650,000 (4).

59           Noroviruses are members of the Caliciviridae family and contain a ~7.5 kb  
60 single stranded, positive polarity RNA genome. They are divided into 5  
61 genogroups; genogroups I and II are responsible for the majority of human  
62 disease and are further subdivided into at least 9 and 22 genotypes, respectively  
63 (5). The human norovirus genome encodes three open reading frames: the non-  
64 structural proteins, the ORF2 major capsid protein (VP1), and the ORF3 minor  
65 capsid protein (VP2) (6). VP1 is further divided into the shell (S) and protruding  
66 (P) domains, with the P domain is comprised of the P1 and P2 subdomains (6).  
67 Phylogenetic studies indicate that the P2 subdomain is the most variable region  
68 of the norovirus genome (7, 8). The P2 subdomain is also the most surface  
69 exposed region of the norovirus capsid, interacting with antibodies and  
70 histoblood group antigens, which serve as binding ligands and putative receptors  
71 for human norovirus docking and entry.

72            GII.4 strains cause over 70% of all norovirus outbreaks (9) and epidemic  
73 outbreaks occur every 2-4 years involving a new antigenically distinct strain (7,  
74 10). Studies of antigenic variation in GII.4 norovirus have shown that the P2  
75 region is involved in strain specific antibody recognition (7, 11, 12), and contains  
76 at least three blockade (potential neutralization) epitopes (13-15). In epidemic  
77 strains, genetic variation in P2 is linked to antigenic changes over time, indicating  
78 that molecular evolution in the P2 subdomain is likely driven by escape from  
79 human herd immunity (12-17).

80            Noroviruses typically cause acute infection in healthy individuals, resulting  
81 in symptomatic infection for 24-48 hours followed by viral shedding for two to four  
82 weeks (18, 19). However, some immunocompromised individuals such as  
83 transplant patients on immunosuppressive drugs, those with primary  
84 immunodeficiencies, cancer patients undergoing chemotherapy, and those with  
85 HIV may develop chronic norovirus infection. Symptomatic infection and viral  
86 shedding in these patients can persist from weeks to years (20-25) and can  
87 result in medical issues such as dehydration and nutrient deficiencies (26),  
88 making development of treatment options for these patients an important priority.  
89 Unfortunately, there are no approved therapeutics or vaccines for controlling  
90 norovirus infections. Attempted methods to control chronic infection have  
91 included treatment with drugs effective against other diarrheal diseases (27),  
92 adjustment of immunosuppressive drug type or dosage (28), and oral or enteral  
93 administration of human IgG (29-32). Although reduction in immunosuppression  
94 coupled with IgG administration has shown promise for some transplant patients,

95 IgG therapy has failed in other studies, and reduction of immunosuppression is  
96 not always possible.

97 Existing studies provide a basis to investigate important questions about  
98 chronic norovirus infection. Although unconfirmed, one recent hypothesis is that  
99 chronically infected norovirus patients may be important sources of infection both  
100 in healthcare settings (33) and as potential reservoirs for new emergent GII.4  
101 norovirus strains (20, 23, 25). Although the fitness and the infectivity of  
102 chronically shed virus is currently unknown, potential accounts of chronic  
103 norovirus shedders involved in hospital outbreaks and transmission of virus to  
104 both immunocompromised and immunocompetent individuals have been  
105 documented (21, 33, 34).

106 Virus capsid sequence and phylogenetic data from chronically infected  
107 patients have found substantial genetic variation over the course of infection in  
108 many, but not all, patients (22, 23, 35). Siebenga et al. found that capsid  
109 mutation rate was linked to immune impairment, suggesting that immune-driven  
110 selection drives evolution in the capsid during chronic infection (35), and explains  
111 differences in evolution depending on level of immunosuppression. Additional  
112 studies have corroborated a role for intra-host immune driven selection by  
113 demonstrating that virus isolated from chronically-infected patients undergoes  
114 positive selection and exhibits higher genetic diversity in the capsid protein than  
115 virus from acutely infected individuals (23, 25). In some chronically infected  
116 patients with GII.4 strain infections, many of the changes occur in blockade

117 epitopes, areas of known or predicted antigenic importance but antigenic  
118 comparisons have not been performed (13-15, 22, 35).

119           In this manuscript, we compare and contrast the antigenic differences  
120 using a panel of polyclonal and monoclonal antibodies and time-ordered VLPs  
121 derived from early (day 1—P.D1) and late (day 302—P.D302) capsid protein  
122 amino acid sequences from a chronically infected immunocompromised patient  
123 (23). Our data demonstrate significant antigenic differences between intra-host  
124 variants that mirrors the degree of variation seen in major successive norovirus  
125 strains, suggesting that chronic norovirus infections can evolve antigenically  
126 unique variants with the potential to seed future norovirus outbreaks.

127

128 **Methods**

129 **Sequences and Structural Homology Models**

130 GenBank (NCBI sequence database) sequences used in this study were  
131 JQ478409.1 (GII.4-2006b) (15), JQ417309 (P\_04.2009 or P.D1) (23), JQ417327  
132 (P\_02.2010 or P.D302) (23), JN595867.1 (GII.4-2009) (15), and JX459908.1  
133 (GII.4-2012) (36), and the VA387 crystal structure is available from the RCSB  
134 Protein Data Bank: identifier 2OBT (37). We refer to originally-named P\_04.2009  
135 as P.D1 and P\_02.2010 as P.D302 for simplicity throughout the manuscript.  
136 Homology models of these sequences were constructed using Modeller (Max-  
137 Planck Institutue for Developmental Biology) and modeled in PyMOL.

138

139 **Production of VRPs.** Virus replicon particles (VRPs) encoding the norovirus  
140 major capsid gene were produced as previously described (38). Briefly,  
141 expression vector pVR21 encodes the VEE genome with the VEE structural  
142 genes replaced with a commercially synthesized norovirus ORF2 gene  
143 (BioBasic) behind the 26S promoter. The VEE-norovirus ORF2 construct and two  
144 separate plasmids expressing either the VEE 3526 E1 and E2 glycoproteins or  
145 VEE 3526 capsid protein were used to make RNA. RNA from all three constructs  
146 was electroporated into BHK cells, and 48 hours later VRPs were harvested and  
147 purified by high speed centrifugation. VRP titers were determined by counting  
148 fluorescent cells detected with FITC-labeled antibody. VLP production from VRPs  
149 and structural integrity was confirmed by EM.

150

151 **Production of VLPs.** VLPs were produced as previously described (13, 15).  
152 Briefly, commercially synthesized norovirus ORF2 (BioBasic) from chronically  
153 infected patient sequence or outbreak strain sequence was cloned into  
154 expression vector pVR21 behind the 26S promotor, and genome length RNAs  
155 were synthesized in vitro using T7 RNA polymerase. RNA from the VEE-ORF2  
156 construct and helper RNAs was electroporated into BHK cells, and 24 hours later  
157 VLPs were harvested and purified by high speed centrifugation. VLP  
158 concentration was determined by BCA Protein Assay (Pierce), and structural  
159 integrity was confirmed for all VLPs by EM.

160

161 **HBGA Binding Assay.** HBGA assays were performed as previously described  
162 (7). Briefly, Avidin coated plates (Pierce) were coated with 10 ug/mL synthetic  
163 biotinylated HBGAs (GlycoTech), followed by addition of 2 ug/mL VLPs. HBGA  
164 binding was detected by strain specific mouse polyclonal sera followed by anti-  
165 mouse IgG-HRP (GE Healthcare) and then One-Step Ultra TMB HRP substrate.  
166 Positive reactivity for each HBGA is defined as an OD 450 nm signal above or  
167 equal to 3X the background binding (background range 0.049-0.066) after  
168 background subtraction.

169

170 **EIAs.** Reactivity with mouse and human mAbs was determined by enzyme-linked  
171 immunoassay (EIA). Plates were coated with 0.5 µg/ml VLP in PBS, and then  
172 two-fold serial dilutions of mAb starting at 1 µg/ml mAb were added. Anti-mouse  
173 or human IgG-HRP (GE Healthcare) followed by One-Step Ultra TMB EIA HRP

174 substrate solution was used for detection. Positive reactivity is defined as a mean  
175 OD 450 nm  $\geq$ 0.2 after background subtraction. Data represent the combination of  
176 three independent trials with each VLP run in duplicate in each trial. Sigmoidal  
177 dose response analysis was performed as previously described (14) using the  
178 reactivity at 1 ug/ml as 100% binding. EC<sub>50</sub> values among VLPs were compared  
179 using One-way ANOVA with Dunnett's post test. P<0.05 was considered  
180 significant. VLPs with maximum reactivity below mean OD 450 nm 0.2 were  
181 assigned a value of zero for graphical representations.

182

### 183 **VLP-Carbohydrate Ligand-Binding Antibody Blockade Assays.**

184 Blockade assays using Pig Gastric Mucin Type III (Sigma Chemicals) were  
185 performed as previously described (14). PGM-bound VLPs were detected by  
186 rabbit anti-GII.4 norovirus polyclonal sera. The percent control binding was  
187 defined as the VLP-ligand binding level in the presence of test antibody or sera  
188 compared to the binding level in the absence of antibody multiplied by 100. All  
189 mAbs and sera were tested for blockade potential at two-fold serial dilutions  
190 ranging from 0.0039 to 2  $\mu$ g/ml (mouse mAbs), 0.0039 to 16  $\mu$ g/ml (human  
191 mAbs), and 0.0098 to 5% (mouse sera). Data from blockade experiments using  
192 monoclonal antibodies represent the combination of three independent trials with  
193 each VLP run in duplicate in each trial. Data from blockade experiments using  
194 polyclonal mouse sera represent the combination of two independent trials in  
195 which sera from five individual mice were tested for each VLP. Sigmoidal dose  
196 response analysis was performed as previously described, and EC<sub>50</sub> values

197 among VLPs were compared using One-way ANOVA with Bonferroni post test.  
198  $P < 0.05$  was considered significant. Blockade assays utilize VLP concentrations  
199 in the low nanomolar range; therefore, this assay does not discriminate between  
200 antibodies with sub-nanomolar affinities.

201

### 202 **Monoclonal antibodies and mouse polyclonal sera**

203 Mouse (12) and human (14) monoclonal antibodies were isolated as previously  
204 described. Balb/c mice (five per group) were immunized by footpad injection with  
205  $5 \times 10^4$  VRPs expressing norovirus capsid gene (GII.4-1987, GII.4-2002, GII.4-  
206 2006b, GII.4-2009, P.D1, or P.D302). Mice were boosted on day 21, euthanized  
207 7 days post-boost, and sera were harvested. This study followed all institutional  
208 guidelines for animal care and experimentation (IACUC guidelines).

209

### 210 **Antigenic Cartography**

211 We utilized multi-dimensional scaling (MDS) approaches as described and  
212 implemented within the AntigenMap 3D software (39, 40). The  $EC_{50}$  blockade  
213 titers of various sera against a panel of VLPs were normalized to maximum  
214 blockade titer of each sera, as well as to the maximum overall blockade titer  
215 across sera (Normalization method 1 in AntigenMap 3D). Normalized values  
216 were used to calculate Euclidean distances,  $D$ , between each pair of VLPs. For  
217 greater analytic, visualization, and graphical purposes, we then utilized  
218 Matlab8.1's (MathWorks Inc, Natick, MA) `cmdscale` function to determine the  
219 XYZ coordinates such that the data can be displayed in 3 dimensions while

220 maintaining the underlying Euclidean distances directly calculated from the data.  
221 We utilized R ([www.r-project.org](http://www.r-project.org)), with the package rgl for 3D visualization of  
222 these data. We confirmed the output of our pipeline with that produced by  
223 AntigenMap 3D.

224 **Results**225 **Comparison of sequence changes among chronic infection isolates GII.4-**  
226 **2006b.**

227 Previous work has shown that changes identified in a few key surface  
228 exposed epitopes correlate with shifts in GII.4 norovirus antigenicity (11, 13-15),  
229 including residues in Epitope A (294, 296-298, 368, and 372) (13), Epitope D  
230 (393-395) (14), and Epitope E (407, 412-413) (15). Changes in these residues  
231 likely alter the ability of preexisting immunity to neutralize the virus, selecting for  
232 the emergence of new epidemic strains.

233 To study the within-host antigenic evolution of noroviruses during a  
234 chronic human infection, we aligned the sequence of the capsid P2 domains of  
235 GII.4-2006b, P.D1, and P.D302 to examine sequential amino acid changes from  
236 GII.4-2006b through P.D302 after at least 10 months of within-host evolution  
237 (23). Note that day 1 and day 302 refer to the days of sample collection and not  
238 from beginning of infection, as the time between the beginning of infection and  
239 the collection of the day 1 sample is unknown. Between VP1 amino acid  
240 positions 248-434, there are 9 differences between GII.4-2006b and P.D1. After  
241 10 months, there were 15 additional differences between P.D1 and P.D302, and  
242 20 differences between GII.4-2006b and P.D302 located between these amino  
243 acid positions (Figure 1A). Similarly, there are 16 differences spanning this  
244 domain between GII.4-2006b and subsequent epidemic strains, GII.4-2009 and  
245 GII.4-2012. Two of the differences between GII.4-2006b and P.D1 (S368A and  
246 S393G) and four of the differences between GII.4-2006b and P.D302 (A294G,

247 S296T, S368A, and N412D) are located within blockade epitope sites (Figure  
248 1B). Four differences in blockade epitope residues also exist between P.D1 and  
249 P.D302 (A294G, S296T, G393S, N412D) (Figure 1B). We synthesized GII.4-  
250 2006b, P.D1, and P.D302 genes, expressed VLPs representing these strains,  
251 and measured differences in antigenicity and HBGA binding among the chronic  
252 infection isolates and GII.4-2006b using biological assays. In addition, several  
253 amino acid substitutions present in the chronic infection strains that are  
254 conserved in past epidemic strains may also influence the antigenic and HBGA  
255 binding characteristics of epitope sites A (292, 295, 373), D (391), and E (414)  
256 (Figure 1B) based on their position relative to these epitopes in GII.4 homology  
257 models (Figure 1C).

#### 258 **Comparison of HBGA binding in chronic infection isolates to GII.4-2006b.**

259 To evaluate differences in HBGA binding preferences among GII.4-2006b,  
260 P.D1, and P.D302, we measured VLP binding to synthetic biotinylated  
261 carbohydrates (A, B, Le<sup>a</sup>, Le<sup>b</sup>, Le<sup>x</sup>, Le<sup>y</sup>, H type 1, and H type 3). As previously  
262 reported, GII.4-2006b bound A, B, Le<sup>b</sup>, Le<sup>y</sup>, and H type 3 (41). In contrast,  
263 chronic infection strain VLPs exhibited differential HBGA binding profiles  
264 compared to GII.4-2006b and to each other (Table 1). P.D1 was able to bind A,  
265 B, and H type 3, while P.D302 bound only B and H type 3 synthetic biotinylated  
266 HBGAs. This indicates that HBGA binding preferences may be altered over time  
267 during chronic infection, perhaps influenced by individual within host HBGA  
268 expression phenotypes.

269

270 **Reactivity with GII.4 Mouse and Human mAbs**

271 To measure antigenic differences among VLPs representing GII.4-2006b  
272 and chronic strains P.D1 and P.D302, we performed enzyme-linked  
273 immunoassays (EIAs) using mouse and human mAbs. We tested five GII.4-  
274 2006b mouse mAbs (G2, G3, G4, G6, G7) and two GII.4 human mAbs (NVB111,  
275 NVB43.9), all of which target epitope site A residues (294, 296-298, 368, and  
276 372), for EIA binding with GII.4-2006b, P.D1, and P.D302 VLPs. GII.4-2006b and  
277 P.D1 differ in one epitope site A position, where P.D1 contains S368A compared  
278 to GII.4-2006b. P.D302 is different from GII.4-2006b at 3/6 epitope site A  
279 residues: A294G, S296T, and S368A, while P.D1 and P.D302 are different at 2/6  
280 epitope site A residues: A294G and S296T. We also tested reactivity of these  
281 VLPs with one human mAb (NVB97), which targets epitope site D residues (393-  
282 395). While GII.4-2006b and P.D302 share identical epitope site D residues,  
283 P.D1 has an S393G change compared to GII.4-2006b. We additionally tested  
284 one human mAb (NVB71.4) that targets an unmapped conserved GII.4 epitope  
285 (14). Consistent with previously-reported results, all mAbs reacted strongly with  
286 GII.4-2006b VLPs (12, 14) (Table 2). In contrast, EC<sub>50</sub> values for P.D1 VLPs  
287 were significantly different ( $P<0.05$ ) from GII.4-2006b VLPs for mouse mAbs G2,  
288 G4, G6, and human mAbs NVB43.9, and NVB111 (Table 2). Moreover, EC<sub>50</sub>  
289 values for P.D302 VLPs were significantly different from GII.4-2006b for all mAbs  
290 except NVB71.4, and different from P.D1 VLPs for all but NVB71.4 and NVB111  
291 (Table 2). This indicates that epitope sites A and D are antigenically distinct

292 among GII.4-2006b, P.D1, and P.D302, demonstrating antigenic variation over  
293 the course of chronic infection in important blockade epitopes.

294

#### 295 **Blockade Activity for GII.4 Mouse and Human mAbs**

296       Compared to EIA, neutralization is a more relevant measure of functional  
297 antigenic change. To test potential neutralization activity of mAbs (GII.4-2006b-  
298 G2, G3, G4, G6, and G7, and NVB43.9, NVB71.4, NVB97, NVB111) against  
299 GII.4-2006b, P.D1, and P.D302 VLPs, we performed blockade assays, a  
300 correlate of protective immunity (42) and a neutralization surrogate. Consistent  
301 with previous findings, all mAbs were able to block ligand-VLP interactions for  
302 GII.4-2006b (12, 14) (Figure 2). Likewise, P.D1 was blocked by all mAbs (Figure  
303 2). However,  $EC_{50}$  blockade titers for two out of five GII.4-2006b mouse mAbs,  
304 G2 (Figure 2A) and G7 (Figure 2E), and two of four GII.4 human mAbs, NVB111  
305 (Figure 2G) and NVB71.4 (Figure 2I), were significantly different, requiring 7.1X,  
306 2X, 2X, 3.2X more antibody, respectively, for blockade compared to GII.4-2006b  
307 VLPs. P.D302 VLP-ligand binding was blocked by GII.4-2006b mouse mAbs G2  
308 (Figure 2A), G6 (Figure 2D), G7 (Figure 2E), but not by G3 (Figure 2B) or G4  
309 (Figure 2C), and blocked by GII.4 human mAb NVB71.4 (Figures 2I), but not by  
310 NVB43.9 (Figure 2F), NVB111 (Figure 2G), or NVB97 (Figures 2H).  $EC_{50}$   
311 blockade titers were significantly different between GII.4-2006b and P.D302 for  
312 G2, G6, G7, and NVB71.4, requiring 12.6X, 15.9X, 12X, and 6.8X more mAb  
313 compared to GII.4-2006b, respectively. Overall,  $EC_{50}$  blockade titers were  
314 significantly higher for P.D302 compared to both GII.4-2006 and P.D1 for all

315 tested mAbs, demonstrating major antigenic changes in epitope sites A and D  
316 over the course of chronic norovirus infection.

317

### 318 **Blockade Response of Strain Specific Mouse Polyclonal Sera**

319 While monoclonal antibodies are informative of the changes in a single  
320 epitope, polyclonal sera are needed to evaluate global antigenic changes. To  
321 measure differences in the total antibody response, we immunized mice with  
322 virus replicon particles (VRPs) expressing the capsid gene from GII.4-2006b,  
323 P.D1, and P.D302 or GII.4-2009, the consecutive outbreak strain following GII.4-  
324 2006, and measured the induced serum blockade responses (Figure 3). Mice  
325 immunized with GII.4-2006b VRPs mounted a robust blockade response against  
326 homotypic GII.4-2006b VLPs, while significantly more sera was needed to block  
327 GII.4-2009, P.D1, and P.D302 VLPs (16X, 9.4X, and 12.7X, respectively) (Figure  
328 3A). Sera from mice immunized with GII.4-2009 VRPs induced a strong  
329 blockade response against GII.4-2009 VLPs; however, significantly more sera  
330 was needed to block GII.4-2006b and P.D302 VLPs, with 39X more sera needed  
331 to block P.D302 VLPs compared to GII.4-2009 (Figure 3B). Sera from mice  
332 immunized with P.D1 VRPs most efficiently blocked homotypic P.D1 VLPs.  $EC_{50}$   
333 values indicated that more sera is required to block GII.4-2009 (3X) and P.D302  
334 (25.8X) than P.D1, while GII.4-2006b and P.D1  $EC_{50}$  titers were not significantly  
335 different (Figure 3C). Sera from mice immunized with P.D302 VRPs efficiently  
336 blocked P.D302 VLP-ligand interactions and weakly blocked GII.4-2006b and  
337 P.D1, requiring 92X and 61X more sera, respectively. P.D302 sera was unable

338 to block GII.4-2009 VLPs (Figure 3D). This data shows that chronic isolate VLPs  
339 induce antibody responses that are different from the parental strain and each  
340 other, demonstrating major changes in total antibody response over the course of  
341 chronic infection.

342

### 343 **Antigenic Cartography**

344 In order to further describe and visualize the differences between virus  
345 strains in their antigenic properties, we utilized the multi-dimensional scaling  
346 (MDS) approach known as antigenic cartography (39,40). Specifically, we used  
347 the pipeline described in AntigenMap 3D (39) to measure and visualize the  
348 antigenic relationships among outbreak strains GII.4-1987, GII.4-1997, GII.4-  
349 2002, GII.4-2006b, GII.4-2009, and GII.4-2012 as well as chronic isolates P.D1  
350 and P.D302, explicitly contrasting antigenic relationships between naturally  
351 occurring epidemic strains as well as intra-host variants. The antigenic distances  
352 between strains were measured using GII.4-1987, GII.4-2002, GII.4-2006b,  
353 GII.4-2009, P.D1, and P.D302 mouse sera EC<sub>50</sub> blocking titers against VLPs  
354 representative of the specified GII.4 strains, and Euclidean distance values were  
355 calculated based on these titers (Figure 4A). Consistent with earlier findings (12),  
356 early (GII.4-1987, GII.4-1997, GII.4-2002) and late strains (GII.4-2006b, GII.4-  
357 2009, GII.4-2012) formed distinct clusters (Figure 4B-C). Not surprisingly, the  
358 early within host variant, P.D1, grouped closely with late strains (Figure 4B-C),  
359 reflecting its origins from the GII.4-2006b lineage. In contrast, P.D302 did not  
360 group with any other strain and was antigenically distant from both the early and

361 contemporary isolates. In order to confirm the visual analysis of these antigenic  
362 similarities, we compared Euclidean distances,  $D$ , between each pair of VLPs  
363 across all serum utilized for antigenic cartography (the Euclidean distance  
364 measures the straight-line distance between two points in a multidimensional  
365 space). We first examined the groupings of early and late GII.4 outbreak strains.  
366 The average distance within a group was 3.79 (range 2.11-6.39) while the  
367 average distance between early and contemporary clusters was 10.7 (range  
368 8.49-13.32), with each distance unit corresponding to a roughly 1.25-fold  
369 difference in blockade response between viruses (Figure 4A). As shown in  
370 Figures 4B and 4C, P.D1 grouped closely with late outbreak strain VLPs, with an  
371 average  $D$  of 3.46 (range 2.26-5.09) (Figure 4A). In contrast, P.D302 was quite  
372 distinct from both early and late outbreak strain viruses, as well as from P.D1,  
373 with an average  $D$  of 9.92 (range 8.73-11.62) (Figure 4A). During an ~10 month  
374 chronic infection in this individual, our data demonstrate that intra-host evolution  
375 can generate novel variants with unique HBGA binding patterns and encode  
376 unique antigenic differences that are as dramatically distinct as time-ordered,  
377 epidemic outbreak strains that emerge in human populations.

378

#### 379 **Expansion of Epitope Site A**

380 We next determined whether novel sites of within host evolution can refine  
381 existing epitope maps and identify potential immunogenic changes in epidemic  
382 strains of the future. Amino acid position 373 exhibited a N373H change between  
383 P.D1 and P.D302 but was conserved in major GII.4 epidemic strains up until a

384 N373R substitution emerged in GII.4-2012 Sydney. Although not supported with  
385 empirical data, recent work by Allen et al (43) suggests that this change in the  
386 Sydney strain may have impacted its emergence. Since changes to 373 have  
387 never been shown to influence immunogenicity, and it is not included as a  
388 diagnostic A epitope site residue, this potentially hampers new epidemic strain  
389 identification. To determine whether position 373 contributes to antigenic  
390 differences in epitope A, we used the blockade assay to test potential  
391 neutralization of VLPs representing parental strains GII.4-2009 New Orleans,  
392 GII.4-2012 Sydney, and chimeric sequences GII.4-2012.09A, GII.4-  
393 2012.09A.R373N, and GII.4-2012.R373N (Figure 5) by epitope A targeting  
394 human mAb 43.9. GII.4-2009 was efficiently blocked by mAb 43.9, while GII.4-  
395 2012 required significantly more (55.3X) mAb for blockade. Blockade response  
396 was partially restored in chimeras GII.4-2012.09A and GII.4-2012.R373N, but  
397 required 1.5X and 4.8X more mAb, respectively, for blockade compared to GII.4-  
398 2009.  $EC_{50}$  blockade titers were not statically different between GII.4-  
399 2012.09A.R373N and GII.4-2009 VLPs. Similar trends were seems using mouse  
400 mAbs targeting epitope A residues (data not shown).

401

## 402 **Discussion**

403 Noroviruses are an important cause of gastroenteritis in  
404 immunocompromised individuals (44, 45), who are at increased risk for severe  
405 disease outcomes (1, 44). Recent vaccine trials utilizing a VLP-based vaccine  
406 approach support the idea that efficacious vaccines can be generated that elicit

407 short term protection in some healthy individuals, but vaccines may not protect  
408 immunocompromised populations, making development of therapeutics that  
409 effectively treat or prevent norovirus infections a top health priority.

410         In immunocompetent people, norovirus infection results in acute disease  
411 outcomes (46). In contrast, immunocompromised individuals can develop  
412 symptomatic disease and high titer viral shedding up to years. Unfortunately, the  
413 literature on specific chronically-infected norovirus patient populations is sparse,  
414 and duration and severity of chronic norovirus infections is likely influenced by  
415 several factors including underlying condition, drug treatment regime, degree of  
416 immunosuppression, and the rate of within host virus evolution, making it difficult  
417 to define the characteristics of a typical chronic norovirus case. From these  
418 limited studies, it is difficult to discern whether there are characteristics of chronic  
419 norovirus infection that are broadly applicable to all populations, characteristics  
420 that are true to specific populations, or whether characteristics vary by each  
421 individual case. Previous work has shown that during the course of chronic  
422 infection, virus genetic diversity can expand quickly (22, 23, 25, 35); however, it  
423 was previously unknown whether this genetic variation translated into antigenic  
424 variation or the emergence of antigenically unique isolates that differ significantly  
425 from contemporary epidemic strains. For the first time, our work clearly  
426 demonstrates the potential for significant antigenic variation over the course of  
427 chronic infection within an individual, which is important in terms of both  
428 therapeutic treatment considerations and for studying the potential role for  
429 chronic shedders as reservoirs for evolving new outbreak strains.

430           Since there is no known animal reservoir for human noroviruses (47), the  
431 available data indicate that new GII.4 strains likely arise naturally within the  
432 human population by epochal evolution, immune driven selection, and inter-host  
433 transmission over time (12-14, 16, 17). The occurrence of frequent long-term  
434 chronic infections in immunosuppressed patients also represents a possible  
435 source of new GII.4 norovirus strains with epidemic potential (23, 25, 35), as  
436 these patients may provide an appropriate environment for sustained immune-  
437 directed molecular evolution by targeting previously identified surface exposed  
438 blockade epitopes for mutation driven escape. Evidence supporting this  
439 hypothesis includes sequence data from chronically infected patients that  
440 demonstrate the emergence of genetic changes in GII.4 blockade epitopes that  
441 modulate inter-host antigenicity (22, 35). This diverse pool may contain variants  
442 antigenically distinct from the predominant circulating strain, allowing emergence  
443 of a new strain under the right conditions (25). However, host and environmental  
444 factors coupled with the type and degree of immunosuppression may affect the  
445 rate and complexity of intra-host evolution that occurs over time (23), and future  
446 work that evaluates the role of different immunosuppressive conditions on intra-  
447 host norovirus evolution are needed.

448           Our work demonstrated intra-host antigenic changes within epitope site A  
449 (amino acids 294, 296-298, 368, and 372). Interestingly, P.D302 contained  
450 residue substitutions in amino acid positions 292, 295, and 373, which are  
451 conserved in major GII.4 outbreak strains, except for 373, which was altered in  
452 the most recent predominant strain, GII.4-2012 Sydney. Changes in these

453 residues likely impact epitope A antibody binding and blockade response either  
454 by altering the conformational landscape of the epitope or directly inhibiting the  
455 interaction of the antibody with the capsid. Using GII.4-2009/GII.4-2012 chimeric  
456 VLPs, we demonstrated that residues at position 373 impact the blockade  
457 response of human mAb NVB 43.9, an antibody that targets epitope A. This  
458 demonstrates that 373 is part of epitope A, expanding this epitope to 7 positions.  
459 Furthermore, we suggest that monitoring intra-host evolved strains may provide a  
460 novel diagnostic strategy to map key residues capable of mediating antigenic  
461 changes in future outbreaks. While positions 292 and 295 have been conserved  
462 in previous predominantly-circulating GII.4 strains, their ability to change in this  
463 patient and their proximity to known epitope A residues suggest that these  
464 residues could potentially impact antigenic change in epitope A in future  
465 epidemics, as residue 373 did in GII.4-2012 Sydney.

466       Reactivity and blockade response data for antibody NVB97 demonstrates  
467 antigenic evolution in epitope site D during chronic infection. Epitope site D  
468 minimally include residues 393-395, is in close proximity to the carbohydrate  
469 binding pocket (37), and previous work demonstrates that modulation of residues  
470 within this epitope modulate HBGA specificity (7). Evolution in this epitope site is  
471 likely driven both by antibody selective pressure and pressure to maintain binding  
472 to one or more HBGAs. Despite conservation of residues 393-395 between  
473 GII.4-2006b and P.D302, antigenic phenotypes differ significantly, demonstrating  
474 that NVB97 recognition is modulated by amino acid positions outside of the  
475 previously-defined epitope site D residues. Position 391, which is close to the

476 carbohydrate binding pocket, is conserved in major outbreak strains and between  
477 GII.4-2006b and P.D1, and previous work demonstrated that an alanine  
478 substitution at this residue had little impact on HBGA binding (48). Neither the  
479 antigenic consequences of residue changes nor the impact of other residue  
480 substitutions on HBGA binding at this position have been rigorously evaluated,  
481 meaning that the D391N change in P.D302 may contribute to both the HBGA  
482 reactivity and antibody blockade differences observed for P.D302. To explore  
483 this possibility, we created homology models of these P2 domains and compared  
484 the predicted polar interactions present in residues 390-395 (Figure 6) among  
485 GII.4-2006b, P.D1, and P.D302.

486 Conformational comparisons between GII.4-2006b and P.D1 show  
487 general similarities in the shape created by residues 390-395, with exceptions  
488 being the loss of a side chain in 393 of P.D1, and slight shifts in position for side  
489 chains in residues 394 and 395 (Figure 6A and 6B). These conformational  
490 changes appear to impact the polar interactions within these residues, as the  
491 loss of the side chain in residue 393 ablates the hydrogen bond present in GII.4-  
492 2006b. In addition, the positional shifts in residues 394 and 395 in P.D1 appear  
493 to prevent formation of another hydrogen bond present in GII.4-2006b.  
494 Conformational comparisons between GII.4-2006b and P.D302 demonstrate that  
495 the residue change at 391 has significant impact on the shape and hydrogen  
496 bonding networks for residues 390-395 (Figures 6A and 6C). In P.D302, position  
497 391 is bent downward, which differs from the position of this amino acid in GII.4-  
498 2006b and P.D1. The result of this change is the formation of a hydrogen bond

499 between the side chain and main chain of 391. In addition, though residue 393 is  
500 conserved between GII.4-2006b and P.D302, the side chain is shifted downward  
501 in P.D302 compared to GII.4-2006b, shifting the position of the hydrogen bond  
502 found at this residue. The formation of two additional novel hydrogen bonds  
503 between 390 & 393 and 390 & 395 suggests that the 391 residue change and  
504 resulting conformational changes allowed for these increased polar interactions.  
505 A slight conformational shift in residue 395 in P.D302 appears to ablate a polar  
506 interaction found in GII.4-2006b at this position. We also compared polar  
507 interactions of GII.4-2006, P.D1, and P.D302 to residues outside of 390-395  
508 (Figure 6D-F). GII.4-2006b and P.D1 displayed five conserved polar interactions  
509 to surrounding amino acids (Figures 6D and 6E), while P.D302 lost the polar  
510 interaction at residue 391 and gained an additional bond at residue 394 (Figure  
511 6F).

512 In addition to epitope site D being an antibody blockade epitope, these  
513 residues modulate HBGA binding, so evolution in this region is likely driven both  
514 by antibody selective pressure and pressure to maintain binding to one or more  
515 HBGAs. Interestingly, all three structures maintained the two hydrogen bonds to  
516 positions 443 and 444. Residue 443 is in the HBGA binding site (37), and  
517 maintaining interaction with this residue may be selected for in this individual in  
518 order to retain HBGA binding. The altered HBGA binding profile and reduced  
519 NBV 97 binding and blockade for P.D302 may be explained by these polar  
520 differences, although this cannot be confirmed without a crystal structure of these  
521 P2 domains bound to NVB 97 and HBGAs.

522           Our demonstration of intra-host changes in HBGA binding profiles in a  
523 chronically infected immunocompromised patient suggests that selection may  
524 favor variants that bind patient-specific HBGAs. While speculative, the potential  
525 emergence of intra-host variants that target patient-specific HBGA expression  
526 profiles could select for the emergence of novel strains that recognize unique or  
527 broad combinations of HBGA patterns, allowing for altered pathogenicity and  
528 transmission efficiencies in an individual or across select human populations. We  
529 could not evaluate this possibility in our study because the HBGA expression  
530 profile of this chronically infected patient is unknown. Future research could  
531 evaluate these HBGA phenotypic and FUT 2/3 genotypic relationships using  
532 saliva and cells from chronically infected patients.

533           How much intra-host and inter-host antigenic variation is necessary to give  
534 rise to a new strain that could escape herd immunity in the general population?  
535 Using blockade  $EC_{50}$  data from mouse sera against GII.4-2006b, GII.4-2009  
536 (representative of a successive outbreak strain), P.D1, and P.D302, we  
537 demonstrate that the antigenic variation between P.D1 and P.D302 is 1.5X  
538 greater than that seen between GII.4-2006b and GII.4-2009. To further address  
539 this question, we used antigenic cartography, which provides easily interpretable  
540 measures and visualization of multidimensional antigenic relationships, and has  
541 previously been used to study antigenic differences in influenza strains (40, 49).  
542 This analysis provided further support for the idea that within-host changes in the  
543 virus can equal or exceed those differences seen across successive outbreak  
544 strains, with the antigenic space between P.D302 and both GII.4-2006b ( $D=9.91$ )

545 and P.D1 ( $D=9.15$ ) being greater than the average between the consecutive  
546 outbreak strains used in this study (average  $D=4.98$ ; range 2.11 to 12.11) and  
547 mirrors the global difference between early GII.4 isolates (1987, 1997, 2002) and  
548 contemporary strains (2006b, 2009, 2012).

549       Antigenic cartography is a relatively new, powerful method with which to  
550 simply describe the multidimensional antigenic differences between virus strains.  
551 As such, there is room for improvement within these methods. Indeed, more  
552 complex statistical models underlying antigenic cartography approaches are  
553 being developed to better account for uncertainty within these datasets (49), and  
554 more comprehensive surveys of both antisera and natural GII.4 isolates over a  
555 30-year time span will better allow for the characterization of antigenic change  
556 within noroviruses. Within this study, the use of mouse sera permits us to use an  
557 immunologically clean background with no pre-exposure history and provides a  
558 clearer starting point to evaluate specific relationships among outbreak strains  
559 and the intra-host isolates. Future work will require well defined, time-ordered  
560 human sera during natural epidemic outbreaks, time-ordered sera during intra-  
561 host chronic infections, and synthetic reconstruction of capsids representing both  
562 outbreak and unique panels of inter-host variants over time; unfortunately, to  
563 date, we have been unable to obtain the samples necessary to pursue this  
564 comprehensive investigation. Our data suggest that intra-host evolution over a  
565 10-month period can yield sufficient antigenic change to escape existing herd  
566 immunity. Clearly, additional work examining norovirus infectivity after prolonged

567 shedding is needed in order to clarify whether chronically infected patients are a  
568 probable source of novel epidemic strains.

569           Therapeutics are needed to alleviate clinical disease during long-term  
570 norovirus infection and prevent the potential emergence of novel antigenic  
571 variants with epidemic potential in the general population. Some success using  
572 IgG to treat chronic norovirus (32) coupled with our data demonstrating that P.D1  
573 is relatively antigenically similar to GII.4-2006b, while P.D302 is antigenically  
574 divergent, suggest that treating early during chronic infection may be important  
575 for viral clearance and also supports the possibility that similarly-administered  
576 broadly neutralizing antibodies may be viable treatment options for patients  
577 suffering from long-term norovirus infection. Our work demonstrates that GII.4  
578 broadly-neutralizing mAb NVB71.4 retains blockade response against P.D1 and  
579 P.D302, even though both these strains are antigenically distinct from GII.4-  
580 2006b, GII.4-2009, and presumably other major GII.4 strains. This suggests that  
581 NVB71.4 or other antibodies with broad cross-blockade activity could be isolated  
582 and successfully used as norovirus therapeutics. Importantly, different  
583 monoclonal antibodies will be needed that target other GI and GII strain chronic  
584 infections. Furthermore, increased surveillance of norovirus isolates from  
585 chronically infected patients as well as deep sequencing of patient isolates  
586 should be considered in order to better understand the transmission dynamics  
587 and genetic potential of norovirus isolates from these patients since these are  
588 likely different from what is seen in the general population. Overall, our work  
589 supports the idea that chronically infected individuals are potential reservoirs for

590 antigenically novel norovirus strains, and further work to characterize their role in  
591 transmission and emergent norovirus outbreaks and development of therapeutics  
592 to combat chronic infections should receive a top priority.

593

#### 594 **Acknowledgements**

595 This work was supported by grant AI056351 from the National Institutes of  
596 Health, Allergy and Infectious Diseases and by institutional training grant T32-  
597 AI007419 from the National Institute of Health. The funders had no role in study  
598 design, data collection and analysis, decision to publish, or preparation of the  
599 manuscript. We thank Victoria Madden and C. Robert Bagnell, Jr., of the  
600 Microscopy Services Laboratory, Department of Pathology and Laboratory  
601 Medicine, University of North Carolina—Chapel Hill, for expert technical support.  
602 We also acknowledge the UNC-CH Genome Analysis Facility.

603

#### 604 **Figure Legends**

##### 605 **Figure 1: Sequence Changes in Chronically Infected Patient Strains**

##### 606 **Compared to GII.4-2006b.**

607 (A) Available capsid amino acid sequences for GII.4-2006b, P.D1 and P.D302  
608 were aligned using Clustal Omega, and sequence differences among GII.4-2006b,  
609 P.D1, and P.D302 are shown. GII.4-2006b residues are shown in purple. P.D1  
610 and P.D302 differences from GII.4-2006b are indicated in light blue, while orange  
611 indicates a reversion to the GII.4-2006b residues. (B) Alignment of GII.4-2006b,

612 P.D1, and P.D302 amino acid sequences in and around Epitopes A, D, and E.  
613 Green indicates a position within a defined epitope, while white indicates nearby  
614 residues that may impact antigenicity in these epitopes. Yellow indicates an  
615 amino acid position newly defined as part of epitope A. (C) Structural homology  
616 models of GII.4-2006b, P.D1, and P.D302 capsid P2 dimers shown from top  
617 view. Purple shows location of Epitopes A, D, and E on the capsid P2 dimer,  
618 while green shows changing amino acid residues in P.D1 and P.D302 compared  
619 to GII.4-2006b.

620

621 **Table 1: Chronic Infection Strain HBGA Binding Preferences**

622 VLPs representing GII.4-2006b, P.D1, and P.D302 were assayed for their ability  
623 to bind synthetic biotinylated HBGAs A, B, Le<sup>a</sup>, Le<sup>b</sup>, Le<sup>x</sup>, Le<sup>y</sup>, H type 1, and H  
624 type 3 by carbohydrate binding assay. Positive reactivity was defined as a value  
625 greater or equal to 3X the background binding value.

626

627 **Table 2: GII.4 Mouse and Human mAb EIA Reactivity with Chronic Infection**

628 **Strains**

629 Mouse and human GII.4 monoclonal antibodies against were assayed for  
630 reactivity with GII.4-2006b, P.D1, and P.D302 VLPs by multiple dilution EIA. The  
631 mean percent binding (percent of the VLP bound to antibody in the dilution  
632 course compared to the amount of VLP bound with antibody at 1 ug/mL) of each  
633 VLP was fit with a sigmoidal curve, and the mean EC<sub>50</sub> (µg/ml) EIA reactivity

634 titers for GII.4-2006b, P.D1, and P.D302 were calculated. \* Mean  $EC_{50}$  EIA  
635 reactivity titer for the test VLP is significantly different from the mean  $EC_{50}$  for  
636 GII.4-2006b (light grey), or \*\* was significantly different from both GII.4-2006b  
637 and P.D1 ( $p < 0.05$ ) (dark grey). Monoclonal antibodies that did not demonstrate  
638 EIA reactivity at or above OD450 nm 0.2 at 1  $\mu\text{g}/\text{mL}$  with a particular VLP are  
639 denoted by an  $EC_{50}$  of  $>1 \mu\text{g}/\text{mL}$ . Statistics were calculated by One-way ANOVA  
640 with Bonferroni post test.

641

642 **Figure 2: GII.4 Mouse and Human mAb Blockade Response Against**  
643 **Chronic Infection Strains**

644 (A-I) Mouse and human GII.4 monoclonal antibodies were assayed for ability to  
645 block GII.4-2006b, P.D1, and P.D302 VLP interaction with carbohydrate ligand.  
646 The mean percent control binding (percent of the VLP bound to carbohydrate  
647 ligand in the presence of an antibody compared to the amount of VLP bound with  
648 no antibody present) of each VLP was fit with a sigmoidal curve, and the mean  
649  $EC_{50}$  ( $\mu\text{g}/\text{ml}$ ) blockade titers for GII.4-2006b, P.D1, and P.D302 were calculated.  
650 Error bars represent 95% confidence intervals. \* Mean  $EC_{50}$  blockade titer for the  
651 test VLP is significantly different from the mean  $EC_{50}$  for GII.4-2006b ( $p < 0.05$ ), or  
652 \*\* was significantly different from both GII.4-2006b and P.D1 ( $p < 0.05$ ).  
653 Monoclonal antibodies that did not block a particular VLP were assigned an  $EC_{50}$   
654 of 2X the upper limit of detection for statistical analysis and are shown on the

655 graph by data points above the upper limit of detection (dashed line). Statistics  
656 were calculated by One-way ANOVA with Bonferroni post test.

657

658 **Figure 3: Blockade Activity of Mouse Polyclonal Sera Against Homotypic**  
659 **and Heterotypic VLPs**

660 Mice were immunized with VRP expressing the capsid gene of GII.4-2006b,  
661 GII.4-2009, P.D1, and P.D302, and sera collected from these mice were tested  
662 for blockade activity against GII.4-2006b, GII.4-2009, P.D1, and P.D302 VLPs.  
663 (A) Blockade activity of sera from mice immunized against GII.4-2006b (A), GII.4-  
664 2009 (B), P.D1 (C), and P.D302 (D) with homotypic and heterotypic VLPs. The  
665 mean percent control binding (percent of the VLP bound to carbohydrate ligand  
666 in the presence of sera compared to the amount of VLP bound with no sera  
667 present) of each VLP was fit with a sigmoidal curve, and the mean  $EC_{50}$  (% sera)  
668 blockade titers for GII.4-2006b, GII.4-2009, P.D1, and P.D302 were calculated.  
669 Error bars represent 95% confidence intervals. \* Mean  $EC_{50}$  blockade titer for the  
670 test VLP is significantly different from the mean  $EC_{50}$  for the homotypic strain  
671 ( $p < 0.05$ ). Sera that did not block a particular VLP were assigned an  $EC_{50}$  of 10%  
672 sera for statistical analysis and are shown on the graph by data points above the  
673 upper limit of detection (dashed line). Statistics were calculated by One-way  
674 ANOVA with Bonferroni post test.

675

676 **Figure 4: Antigenic Cartography for GII.4 Noroviruses**

677 Multidimensional Scaling (MDS) was used to identify the antigenic relationships  
678 between different norovirus strains. A) Euclidean antigenic distances between  
679 virus strains were calculated based on the EC<sub>50</sub> efficacy of antisera raised  
680 against GII.4-1987, GII.4-2002, GII.4-2006b, GII.4-2009, P.D1 and P.D302 VLPs.  
681 Green squares represent distances within either the early (1987, 1998 and 2002)  
682 or late (2006, 2009 and 2012) virus groups. Purple squares show the distances  
683 between early and late virus groups. (B-C) We determined XYZ-coordinates that  
684 maintain the underlying Euclidean distances between viruses, while illustrating  
685 the relationships between GII.4 norovirus strains, with each map-distance  
686 roughly corresponding to a ~1.25-fold change in blockade response. B) Early  
687 strains GII.4-1987 (yellow), GII.4-1997 (red), and GII.4-2002 (light blue) grouped  
688 together (lower right hand group), and late strains GII.4-2006b (light purple),  
689 GII.4-2009 (dark blue), and GII.4-2012 (dark purple) grouped together (lower left  
690 hand group). P.D1 grouped with late strains, closest to GII.4-2006b, while  
691 P.D302 was separate from either late or early strains (upper position). C) Side  
692 view of the same 3D graph showing the antigenic differences between strains.

693

694 **Figure 5: Expansion of Epitope Site A**

695 Epitope A targeting human GII.4 mAb 43.9 was assayed for its ability to block  
696 GII.4-2009 New Orleans, GII.4-2012 Sydney, GII.4-2012.09A, GII.4-2012.R373N,  
697 and GII.4-2012.09A.R373N VLP interaction with carbohydrate ligand. The mean  
698 percent control binding (percent of the VLP bound to carbohydrate ligand in the  
699 presence of an antibody compared to the amount of VLP bound with no antibody

700 present) of each VLP was fit with a sigmoidal curve, and the mean EC<sub>50</sub> (µg/ml)  
 701 blockade titers for all VLPs were calculated. Error bars represent 95% confidence  
 702 intervals. Statistics were calculated by One-way ANOVA with Dunnett's post  
 703 test. \* Mean EC<sub>50</sub> blockade titer was significantly different from GII.4-2009.

704

705 **Figure 6: Comparison of Epitope Site D Polar Interactions Among GII.4-**  
 706 **2006 and Chronic Infection Strains**

707 Pymol was used to model the polar interactions within residues 390-395 (A-C)  
 708 and interactions between these residues and surrounding residues (D-F). GII.4-  
 709 2006b is shown in purple (A and D), P.D1 is shown in teal (B and E), and P.D302  
 710 is shown in pink (C and F). Residues 390-395 are shown in orange for GII.4-  
 711 2006b, yellow for P.D1, and aqua for P.D302. Dotted lines represent structure-  
 712 based predicted polar interactions. Dark purple residues represent positions that  
 713 interact with HBGAs (D-F).

714

715 **References**

716

717

- 718 1. Mattner F, Sohr D, Heim A, Gastmeier P, Vennema H, Koopmans M. 2006. Risk  
 719 groups for clinical complications of norovirus infections: an outbreak  
 720 investigation. *Clin Microbiol Infect* 12:69-74.
- 721 2. Murata T, Katsushima N, Mizuta K, Muraki Y, Hongo S, Matsuzaki Y. 2007.  
 722 Prolonged norovirus shedding in infants <or=6 months of age with  
 723 gastroenteritis. *Pediatr Infect Dis J* 26:46-49.
- 724 3. Okada M, Tanaka T, Oseto M, Takeda N, Shinozaki K. 2006. Genetic analysis of  
 725 noroviruses associated with fatalities in healthcare facilities. *Arch Virol*  
 726 151:1635-1641.

- 727 4. Johnston CP, Qiu H, Ticehurst JR, Dickson C, Rosenbaum P, Lawson P, Stokes  
728 AB, Lowenstein CJ, Kaminsky M, Cosgrove SE, Green KY, Perl TM. 2007.  
729 Outbreak management and implications of a nosocomial norovirus outbreak.  
730 Clin Infect Dis 45:534-540.
- 731 5. Kroneman A, Vega E, Vennema H, Vinje J, White PA, Hansman G, Green K,  
732 Martella V, Katayama K, Koopmans M. 2013. Proposal for a unified norovirus  
733 nomenclature and genotyping. Arch Virol 158:2059-2068.
- 734 6. Prasad BV, Hardy ME, Dokland T, Bella J, Rossmann MG, Estes MK. 1999. X-  
735 ray crystallographic structure of the Norwalk virus capsid. Science 286:287-  
736 290.
- 737 7. Lindesmith LC, Donaldson EF, Lobue AD, Cannon JL, Zheng DP, Vinje J, Baric  
738 RS. 2008. Mechanisms of GII.4 norovirus persistence in human populations.  
739 PLoS Med 5:e31.
- 740 8. Donaldson EF, Lindesmith LC, Lobue AD, Baric RS. 2008. Norovirus  
741 pathogenesis: mechanisms of persistence and immune evasion in human  
742 populations. Immunol Rev 225:190-211.
- 743 9. Fankhauser RL, Monroe SS, Noel JS, Humphrey CD, Bresee JS, Parashar UD,  
744 Ando T, Glass RI. 2002. Epidemiologic and molecular trends of "Norwalk-like  
745 viruses" associated with outbreaks of gastroenteritis in the United States. J  
746 Infect Dis 186:1-7.
- 747 10. Siebenga JJ, Vennema H, Renckens B, de Bruin E, van der Veer B, Siezen RJ,  
748 Koopmans M. 2007. Epochal evolution of GGII.4 norovirus capsid proteins  
749 from 1995 to 2006. J Virol 81:9932-9941.
- 750 11. Allen DJ, Noad R, Samuel D, Gray JJ, Roy P, Iturriza-Gomara M. 2009.  
751 Characterisation of a GII-4 norovirus variant-specific surface-exposed site  
752 involved in antibody binding. Virol J 6:150.
- 753 12. Lindesmith LC, Donaldson EF, Baric RS. 2011. Norovirus GII.4 strain  
754 antigenic variation. J Virol 85:231-242.
- 755 13. Debbink K, Donaldson EF, Lindesmith LC, Baric RS. 2012. Genetic mapping of  
756 a highly variable norovirus GII.4 blockade epitope: potential role in escape  
757 from human herd immunity. J Virol 86:1214-1226.
- 758 14. Lindesmith LC, Beltramello M, Donaldson EF, Corti D, Swanstrom J, Debbink  
759 K, Lanzavecchia A, Baric RS. 2012. Immunogenetic mechanisms driving  
760 norovirus GII.4 antigenic variation. PLoS Pathog 8:e1002705.
- 761 15. Lindesmith LC, Debbink K, Swanstrom J, Vinje J, Costantini V, Baric RS,  
762 Donaldson EF. 2012. Monoclonal antibody-based antigenic mapping of  
763 norovirus GII.4-2002. J Virol 86:873-883.
- 764 16. Lindesmith LC, Costantini V, Swanstrom J, Debbink K, Donaldson EF, Vinje J,  
765 Baric RS. 2013. Emergence of a norovirus GII.4 strain correlates with changes  
766 in evolving blockade epitopes. J Virol 87:2803-2813.
- 767 17. Debbink K, Lindesmith LC, Donaldson EF, Costantini V, Beltramello M, Corti  
768 D, Swanstrom J, Lanzavecchia A, Vinje J, Baric RS. 2013. Emergence of New  
769 Pandemic GII.4 Sydney Norovirus Strain Correlates with Escape from Herd  
770 Immunity. J Infect Dis.

- 771 18. Rockx B, De Wit M, Vennema H, Vinje J, De Bruin E, Van Duynhoven Y,  
772 Koopmans M. 2002. Natural history of human calicivirus infection: a  
773 prospective cohort study. *Clin Infect Dis* 35:246-253.
- 774 19. Obara M, Hasegawa S, Iwai M, Horimoto E, Nakamura K, Kurata T, Saito N, Oe  
775 H, Takizawa T. 2008. Single base substitutions in the capsid region of the  
776 norovirus genome during viral shedding in cases of infection in areas where  
777 norovirus infection is endemic. *J Clin Microbiol* 46:3397-3403.
- 778 20. Siebenga J, Kroneman A, Vennema H, Duizer E, Koopmans M. 2008. Food-  
779 borne viruses in Europe network report: the norovirus GII.4 2006b (for US  
780 named Minerva-like, for Japan Kobe034-like, for UK V6) variant now  
781 dominant in early seasonal surveillance. *Euro Surveill* 13.
- 782 21. Nilsson M, Hedlund KO, Thorhagen M, Larson G, Johansen K, Ekspong A,  
783 Svensson L. 2003. Evolution of human calicivirus RNA in vivo: accumulation  
784 of mutations in the protruding P2 domain of the capsid leads to structural  
785 changes and possibly a new phenotype. *J Virol* 77:13117-13124.
- 786 22. Schorn R, Hohne M, Meerbach A, Bossart W, Wuthrich RP, Schreier E, Muller  
787 NJ, Fehr T. 2010. Chronic norovirus infection after kidney transplantation:  
788 molecular evidence for immune-driven viral evolution. *Clin Infect Dis*  
789 51:307-314.
- 790 23. Hoffmann D, Hutzenthaler M, Seebach J, Panning M, Umgelter A, Menzel H,  
791 Protzer U, Metzler D. 2012. Norovirus GII.4 and GII.7 capsid sequences  
792 undergo positive selection in chronically infected patients. *Infect Genet Evol*  
793 12:461-466.
- 794 24. Ludwig A, Adams O, Laws HJ, Schrotten H, Tenenbaum T. 2008. Quantitative  
795 detection of norovirus excretion in pediatric patients with cancer and  
796 prolonged gastroenteritis and shedding of norovirus. *J Med Virol* 80:1461-  
797 1467.
- 798 25. Bull RA, Eden JS, Luciani F, McElroy K, Rawlinson WD, White PA. 2012.  
799 Contribution of intra- and interhost dynamics to norovirus evolution. *J Virol*  
800 86:3219-3229.
- 801 26. Koo HL, DuPont HL. 2009. Noroviruses as a potential cause of protracted and  
802 lethal disease in immunocompromised patients. *Clin Infect Dis* 49:1069-  
803 1071.
- 804 27. Capizzi T, Makari-Judson G, Steingart R, Mertens WC. 2011. Chronic diarrhea  
805 associated with persistent norovirus excretion in patients with chronic  
806 lymphocytic leukemia: report of two cases. *BMC Infect Dis* 11:131.
- 807 28. Boillat Blanco N, Kuonen R, Bellini C, Manuel O, Estrade C, Mazza-Stalder J,  
808 Aubert JD, Sahli R, Meylan P. 2011. Chronic norovirus gastroenteritis in a  
809 double hematopoietic stem cell and lung transplant recipient. *Transpl Infect*  
810 *Dis* 13:213-215.
- 811 29. Florescu DF, Hill LA, McCartan MA, Grant W. 2008. Two cases of Norwalk  
812 virus enteritis following small bowel transplantation treated with oral  
813 human serum immunoglobulin. *Pediatr Transplant* 12:372-375.
- 814 30. Florescu DF, Hermsen ED, Kwon JY, Gumeel D, Grant WJ, Mercer DF, Kalil AC.  
815 2011. Is there a role for oral human immunoglobulin in the treatment for

- 816 norovirus enteritis in immunocompromised patients? *Pediatr Transplant*  
 817 15:718-721.
- 818 31. Ebdrup L, Bottiger B, Molgaard H, Laursen AL. 2011. Devastating diarrhoea in  
 819 a heart-transplanted patient. *J Clin Virol* 50:263-265.
- 820 32. Chagla Z, Quirt J, Woodward K, Neary J, Rutherford C. 2013. Chronic  
 821 norovirus infection in a transplant patient successfully treated with enterally  
 822 administered immune globulin. *J Clin Virol*.
- 823 33. Sukhrie FH, Siebenga JJ, Beersma MF, Koopmans M. 2010. Chronic shedders  
 824 as reservoir for nosocomial transmission of norovirus. *J Clin Microbiol*  
 825 48:4303-4305.
- 826 34. Kaufman SS, Chatterjee NK, Fuschino ME, Morse DL, Morotti RA, Magid MS,  
 827 Gondolesi GE, Florman SS, Fishbein TM. 2005. Characteristics of human  
 828 calicivirus enteritis in intestinal transplant recipients. *J Pediatr Gastroenterol*  
 829 *Nutr* 40:328-333.
- 830 35. Siebenga JJ, Beersma MF, Vennema H, van Biezen P, Hartwig NJ, Koopmans M.  
 831 2008. High prevalence of prolonged norovirus shedding and illness among  
 832 hospitalized patients: a model for in vivo molecular evolution. *J Infect Dis*  
 833 198:994-1001.
- 834 36. Eden JS, Tanaka MM, Boni MF, Rawlinson WD, White PA. 2013.  
 835 Recombination within the pandemic norovirus GII.4 lineage. *J Virol* 87:6270-  
 836 6282.
- 837 37. Cao S, Lou Z, Tan M, Chen Y, Liu Y, Zhang Z, Zhang XC, Jiang X, Li X, Rao Z.  
 838 2007. Structural basis for the recognition of blood group trisaccharides by  
 839 norovirus. *J Virol* 81:5949-5957.
- 840 38. Baric RS, Yount B, Lindesmith L, Harrington PR, Greene SR, Tseng FC, Davis  
 841 N, Johnston RE, Klapper DG, Moe CL. 2002. Expression and self-assembly of  
 842 norwalk virus capsid protein from venezuelan equine encephalitis virus  
 843 replicons. *J Virol* 76:3023-3030.
- 844 39. Barnett JL, Yang J, Cai Z, Zhang T, Wan XF. 2012. AntigenMap 3D: an online  
 845 antigenic cartography resource. *Bioinformatics* 28:1292-1293.
- 846 40. Cai Z, Zhang T, Wan XF. 2010. A computational framework for influenza  
 847 antigenic cartography. *PLoS Comput Biol* 6:e1000949.
- 848 41. Cannon JL, Lindesmith LC, Donaldson EF, Saxe L, Baric RS, Vinje J. 2009. Herd  
 849 immunity to GII.4 noroviruses is supported by outbreak patient sera. *J Virol*  
 850 83:5363-5374.
- 851 42. Reeck A, Kavanagh O, Estes MK, Opekun AR, Gilger MA, Graham DY, Atmar  
 852 RL. 2010. Serological correlate of protection against norovirus-induced  
 853 gastroenteritis. *J Infect Dis* 202:1212-1218.
- 854 43. Allen DJ, Adams NL, Aladin F, Harris JP, Brown DW. 2014. Emergence of the  
 855 GII-4 Norovirus Sydney2012 Strain in England, Winter 2012-2013. *PLoS One*  
 856 9:e88978.
- 857 44. Roddie C, Paul JP, Benjamin R, Gallimore CI, Xerry J, Gray JJ, Peggs KS, Morris  
 858 EC, Thomson KJ, Ward KN. 2009. Allogeneic hematopoietic stem cell  
 859 transplantation and norovirus gastroenteritis: a previously unrecognized  
 860 cause of morbidity. *Clin Infect Dis* 49:1061-1068.

- 861 45. Glass RI, Parashar UD, Estes MK. 2009. Norovirus gastroenteritis. *N Engl J*  
862 *Med* 361:1776-1785.
- 863 46. Atmar RL, Opekun AR, Gilger MA, Estes MK, Crawford SE, Neill FH, Graham  
864 DY. 2008. Norwalk virus shedding after experimental human infection.  
865 *Emerg Infect Dis* 14:1553-1557.
- 866 47. Etherington GJ, Ring SM, Charleston MA, Dicks J, Rayward-Smith VJ, Roberts  
867 IN. 2006. Tracing the origin and co-phylogeny of the caliciviruses. *J Gen Virol*  
868 87:1229-1235.
- 869 48. Tan M, Xia M, Cao S, Huang P, Farkas T, Meller J, Hegde RS, Li X, Rao Z, Jiang X.  
870 2008. Elucidation of strain-specific interaction of a GII-4 norovirus with  
871 HBGA receptors by site-directed mutagenesis study. *Virology* 379:324-334.
- 872 49. Bedford T, Suchard MA, Lemey P, Dudas G, Gregory V, Hay AJ, McCauley JW,  
873 Russell CA, Smith DJ, Rambaut A. 2014. Integrating influenza antigenic  
874 dynamics with molecular evolution. *Elife* 3:e01914.  
875  
876

	A	B	Le <sup>a</sup>	Le <sup>b</sup>	Le <sup>x</sup>	Le <sup>y</sup>	H type 1	H type 3
GII.4-2006	+	+	-	+	-	+	-	+
P.D1	+	+	-	-	-	-	-	+
P.D302	-	+	-	-	-	-	-	+

**Table 1: Chronic Infection Strain HBGA Binding Preferences**

VLPs representing GII.4-2006b, P.D1, and P.D302 were assayed for their ability to bind synthetic biotinylated HBGAs A, B, Le<sup>a</sup>, Le<sup>b</sup>, Le<sup>x</sup>, Le<sup>y</sup>, H type 1, and H type 3 by carbohydrate binding assay. Positive reactivity was defined as a value greater or equal to 3X the background binding value.

mAb	Epitope Targeted	Mean EC <sub>50</sub> (Upper/Lower Limit)		
		GII.4-2006	P.D1	P.D302
GII.4-2006-G2	A	0.113 (0.130/0.098)	0.290* (0.357/0.235)	>1.00**
GII.4-2006-G3	A	0.097 (0.110/0.085)	0.127 (0.156/0.104)	>1.00**
GII.4-2006-G4	A	0.011 (0.013/0.008)	0.028* (0.045/0.017)	>1.00**
GII.4-2006-G6	A	0.024 (0.029/0.021)	0.052* (0.067/0.040)	0.201** (0.232/0.175)
GII.4-2006-G7	A	0.021 (0.026/0.017)	0.02 (0.027/0.015)	>1.00**
NVB43.9	A	0.024 (0.026/0.022)	0.046* (0.051/0.041)	>1.00**
NVB111	A	0.147 (0.211/0.103)	>1.00*	>1.00*
NVB97	D	0.082 (0.131/0.052)	0.059 (0.084/0.041)	>1.00**
NVB71.4	conserved GII.4	0.151 (0.182/0.125)	0.129 (0.176/0.095)	0.13 (0.168/0.101)

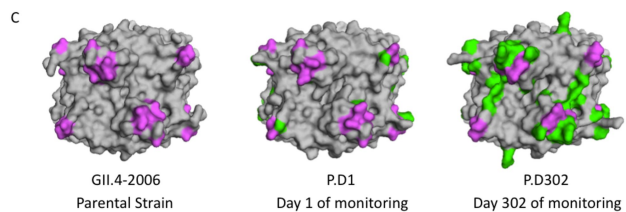
**Table 2: GII.4 Mouse and Human mAb EIA Reactivity with Chronic Infection Strains**  
 Mouse and human GII.4 monoclonal antibodies against were assayed for reactivity with GII.4-2006b, P.D1, and P.D302 VLPs by multiple dilution EIA. The mean percent binding (percent of the VLP bound to antibody in the dilution course compared to the amount of VLP bound with antibody at 1 ug/mL) of each VLP was fit with a sigmoidal curve, and the mean EC<sub>50</sub> (μg/ml) EIA reactivity titers for GII.4-2006b, P.D1, and P.D302 were calculated. \* Mean EC<sub>50</sub> EIA reactivity titer for the test VLP is significantly different from the mean EC<sub>50</sub> for GII.4-2006b (light grey), or \*\* was significantly different from both GII.4-2006b and P.D1 (p<0.05) (dark grey). Monoclonal antibodies that did not demonstrate EIA reactivity at or above OD450 nm 0.2 at 1 ug/mL with a particular VLP are denoted by an EC<sub>50</sub> of >1 ug/mL. Statistics were calculated by One-way ANOVA with Bonferroni post test.

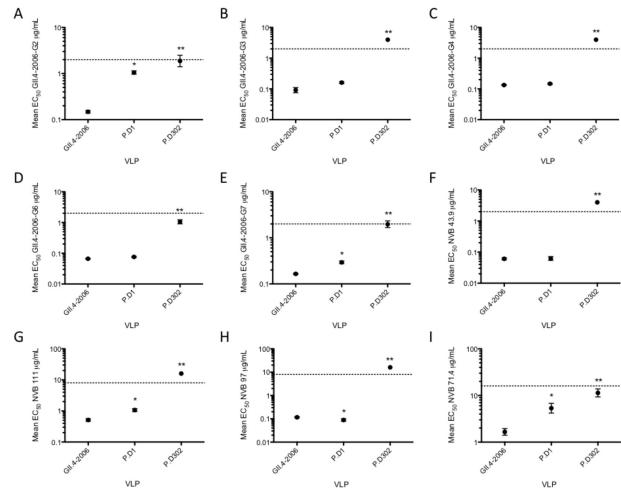
A

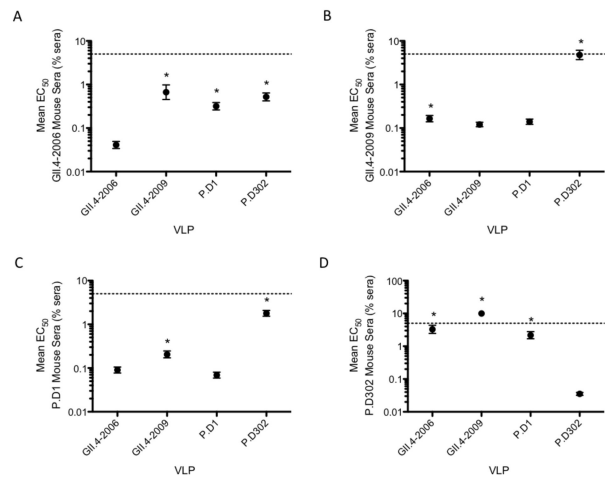
	248	255	271	292	294	295	296	329	340	348	352	356	368	373	391	393	404	412	414	425	426	434
GII.4-2006	K	G	V	H	A	G	S	K	G	K	Y	A	S	N	D	S	V	N	H	T	F	F
P.D1	R	S	M	H	A	G	S	K	G	K	Y	A	A	N	D	G	A	N	Q	N	S	F
P.D302	R	S	M	Q	G	S	T	R	R	T	S	V	A	H	N	S	V	D	Q	N	S	S

B

	A							D			E						
	292	294	295	296	297	298	368	372	373	391	393	394	395	404	407	412	414
GII.4-2006	R	A	G	S	R	N	S	E	N	D	S	T	T	V	S	N	H
P.D1	H	A	G	S	R	N	A	E	N	D	G	T	T	A	S	N	Q
P.D302	Q	G	S	T	R	N	A	E	H	N	S	T	T	V	S	D	Q







**A**

**Antigenic Distances Between Viruses**

	Virus isolate							
	1997	2002	2006	2009	2012	PD1	PD302	
1987	2.11	3.34	12.21	10.07	8.64	11.18	10.34	
1997		3.53	13.32	11.39	10.14	12.38	11.62	
2002			12.11	9.94	8.49	11.06	10.22	
2006				4.26	6.39	3.04	9.91	
2009					3.14	2.26	9.44	
2012						5.09	8.73	
PD1							9.15	

